Lattice dynamics and specific heat of α-GeTe: Theoretical and experimental study

R. Shaltaf and X. Gonze

European Theoretical Spectroscopic Facility, Unit PCPM, Université Catholique de Louvain, B-1348 Louvain-la-Neuve, Belgium

M. Cardona, R. K. Kremer,[*] and G. Siegle

Max-Planck-Institut für Festkörperforschung, Heisenbergstrasse 1, D-70569 Stuttgart, Germany

(Received 24 October 2008; published 13 February 2009)

We extend recent *ab initio* calculations of the electronic band structure and the phonon-dispersion relations of rhombohedral GeTe to calculations of the density of phonon states and the temperature-dependent specific heat. The results are compared to measurements of the specific heat. It is discovered that the specific heat depends on hole concentration, not only in the very low temperature region (Sommerfeld term) but also at the maximum of C_p/T^3 (around 16 K). To explain this phenomenon, we have performed *ab initio* lattice-dynamical calculations for GeTe rendered metallic through the presence of a heavy-hole concentration ($p \sim 2 \times 10^{21}$ cm^{-3}). They account for the increase observed in the maximum of C_p/T^3.

I. INTRODUCTION

GeTe is a material with ten valence electrons per primitive unit cell (PC) and is thus related to the lead chalcogenides PbX (X=S,Se,Te) and to the semimetals As, Sb, and Bi. Like PbX, GeTe is a semiconductor but crystallizes in the rocksalt structure only at temperatures above $\sim$700 K.[1] Below $\sim$650 K, GeTe distorts through an extension of the cube diagonal into a rhombohedral structure[2] similar to that of the semimetals As, Sb, and Bi, except that the two atoms per PC are not equal and hence its bonding is polar. Compatible with the rhombohedral symmetry represented by a strain along [111], there are two additional independent distortion parameters: the rhombohedral angle α, whose distortion from the 60° of the cubic phase brings it to $\approx$58°, and a change in the Ge-Te sublattice separation $a_0\tau\sqrt{3}$ with $\tau \sim 0.03$.[1,3]

This distortion converts GeTe into a ferroelectric with $T_c \sim 650$ K, given the polar nature of the bond. Another interesting property of GeTe is its native p-type doping, with hole concentrations typically higher than 5×10^{19} cm^{-3}. This fact is attributed to the presence of Ge vacancies.[4,5]

The metallic nature of GeTe with high hole concentration ($p > 8.3 \times 10^{20}$) leads to superconductivity at temperatures T_c below $\sim$0.3 K.[5] Finegold[6] examined the heat capacity of a GeTe sample with $p \sim 1.1 \times 10^{21}$ cm^{-3} and $T_c \sim 0.25$ K in the region around T_c and observed the peak related to superconducting behavior: application of a magnetic field of 500 Oe completely wiped out superconductivity and the related peak, thus allowing him to determine, for his sample, a Sommerfeld term $\gamma = 1.32$ mJ/mole K^2. The specific-heat measurements reported here were performed from 4 to 250 K and therefore do not address the superconducting behavior of GeTe. They allow us, however, to determine γ and the maximum in C_p/T^3 (at $\sim$17 K) which signals deviations from Debye's T^3 law. We find this maximum to be 5.5% higher than that obtained from the data of Bevolo *et al.*,[4] a fact that suggests a decrease in phonon frequencies induced by the presence of hole doping whose concentration is, in our sample, $\sim$25 times higher than in that of Bevolo *et al.*[4]

In order to test this hypothesis we have performed *ab initio* calculations of the lattice dynamics of α-GeTe similar to those reported earlier for PbS (Ref. 7) and for PbS, PbSe, and PbTe.[8] Comparison of theoretically obtained without spin-orbit (SO) coupling and experimental values of C_p/T^3 presented in Ref. 7 suggested that there may be a significant contribution ($\sim$20%) of the SO interaction to the value of C_p/T^3 at its maximum [note that in the region of the maximum $C_p \approx C_v$ (Ref. 9)].

We therefore repeated in Ref. 8 lattice-dynamical calculations for PbS, PbSe, and PbTe, this time with and without SO interaction. We were able to prove that the lack of SO interaction, especially at the Pb ions, was largely responsible for the discrepancy just mentioned. In the calculations reported here for α-GeTe we have checked the effect of SO interaction and, not unexpectedly (heavy Pb ions are not present), we found it to be rather small ($\sim$1%); it can thus be neglected in the remaining parts of this work. We did find, however, for the calculated values of C_p/T^3 an increase in its maximum between an undoped sample and one with $p \sim 2.1 \times 10^{21}$ cm^{-3} of $\sim$6%, which largely explains the difference found between our sample and that of Bevolo *et al.*[4] (3.5%). Our calculations of the lattice dispersion relations for $p \sim 2.1 \times 10^{21}$ cm^{-3} and for undoped samples show indeed that the phonon frequencies decrease with doping. This effect is very large around the Γ point of the Brillouin zone (BZ) due to the screening of the ionic charge by the holes. However, it amounts to a few percent throughout most of the BZ.

As a byproduct we have also calculated the phonon density of states (DOS) and its projection on each of the constituent ions. We have also calculated the density of two-phonon states which applies to optical spectroscopies involving two phonons: second-order Raman scattering and infrared absorption. It is hoped that the availability of these DOS calculations will encourage such optical measurements in this interesting material.

II. THEORETICAL DETAILS

All the calculations have been performed using plane waves and norm-conserving pseudopotentials, as imple-

TABLE I. Calculated structural parameters of GeTe. The lattice parameter a_0 (in Å), the angle α (in deg), the deviation from of the Ge sublattice from the 0.5 sublattice position τ, and the volume $\Omega = (a_0^3/4)\sin^2 \alpha$ (in Å³).

	a_0	α	τ	Ω
With SO	5.897	88.96	0.0237	51.26
Without SO	5.894	88.96	0.0237	51.19
Theory[a]	5.886	89.24	0.0217	50.96
Expt.[b]	5.996	88.18	0.026	53.84
Expt.[c]	5.98	88.35	0.0248	53.31

[a]Reference 19.
[b]Reference 3.
[c]Reference 20.

mented in the ABINIT code.[10,11] The dynamical properties have been evaluated within the density-functional perturbation theory.[12–14] We employed Hartwigsen-Goedecker-Hutter (HGH) pseudopotentials,[15] generated including spin-orbit coupling, within the local-density approximation (LDA) adopting the Teter-Pade parameterization.[16] Even though HGH pseudopotentials are known as being relatively hard, the properties investigated in this work are well converged when including a plane-wave basis up to a kinetic-energy cutoff equal to 15 Ha. The Brillouin-zone integration was performed using special **k** points sampled within the Monkhorst-Pack scheme.[17] We found that a mesh of $12 \times 12 \times 12$ **k** points was required to describe well the structural and vibrational properties. Further details on the theoretical calculations are mostly given in Ref. 8 except those for the heavily *p*-doped material which were only performed without SO interaction.

To mimic the effect of Ge vacancies on the calculated force constants, and consequently on the heat capacity, the number of total electrons was reduced by a certain amount δe. The value of δe was chosen to be equivalent to the concentration of the free holes *p*. In all calculations of hole doped cases, (i) a uniform background of negative charge was imposed to achieve charge neutrality and (ii) the first-order Hermite-Gaussian smearing technique of Methfessel and Paxton[18] was employed in the Brillouin-zone integration procedure. We found that a combination of $12 \times 12 \times 12$ **k** points and a smearing value of 0.01 Ha was sufficient for both total energy and structural parameter convergence. Changing the smearing value from 0.01 to 0.005 Ha leads to a change smaller than 1 cm⁻¹ in the phonon frequencies.

Before calculating the dynamical matrix the structural parameters a_0, a, and τ were optimized. In Table I we show the calculated structural parameters with and without SO coupling. The effect of the SO interaction on the structural parameters is found to be negligible. Our results are globally in good agreement with previously reported *ab initio* results.[19] Moreover the deviation between the calculated structural parameters (a_0, α) and experiment is less than 2%.

Although the present methodology is inadequate to compute the effect of the vacancies on the structural parameters (in this case, real vacancies should actually be explicitly treated and not replaced by a change of the number of elec-
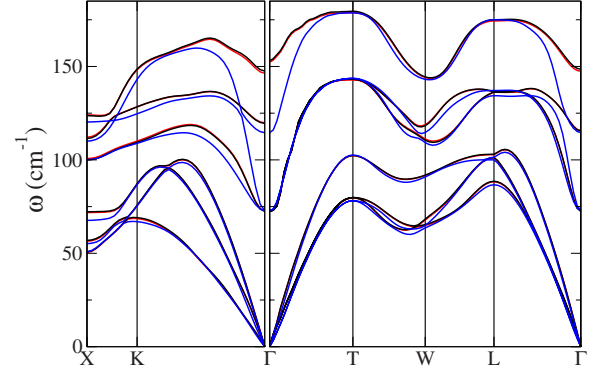

FIG. 1. (Color online) Calculated phonon-dispersion relations of GeTe along selected symmetry directions in the BZ. The (black) solid line denotes the results for stoichiometric undoped GeTe, the (red) solid line denotes the results including spin-orbit coupling, and the (blue) solid line was obtained for doped GeTe with $p=2 \times 10^{21}$ holes/cm³ without spin-orbit coupling.

trons counterbalanced by a background), we have tested the effect of the hole concentration on the structural parameters. For a hole concentration, $p=2.1 \times 10^{21}$ holes/cm³, the structural parameters a_0, α, and τ are 5.765 Å, 89.04°, and 0.0167, respectively, with a unit-cell volume reduced to 47.88 Å³. Such change of structural parameters is not observed in reality: the presence of vacancies affects directly the volume of the sample and seems to act, experimentally, in such a way as to keep the average lattice parameter nearly unchanged with hole concentration. While keeping the average lattice parameter fixed, we have also explored the bulk modulus. We observe a softening of the crystal, the bulk modulus changing from 45.5 GPa (zero doping) to 38.2 GPa ($p=2.1 \times 10^{21}$ holes/cm³ doping). However, also for the bulk modulus, the present approach would be questionable although the decrease with doping correlates with the decrease observed in the acoustic phonon frequencies. We performed the calculations using the parameters obtained without spin-orbit coupling for all cases including those of doped samples.

III. CALCULATED DISPERSION RELATIONS AND PHONON DENSITY OF STATES

In Fig. 1 we show the phonon-dispersion relations calculated for undoped GeTe ($p=0$) and for GeTe containing $p=2.1 \times 10^{21}$ holes/cm³. The undoped material, to the best of our knowledge, has never been prepared. We calculate it as a reference point to assess the effects of *p*-type doping on the dispersion relations. For $p=0$ we have performed calculations without and with SO interaction. This interaction has a very weak effect, only sizeable near the Γ point of the BZ. The frequency of the LO phonons near Γ is lowered by 1.3 cm⁻¹ when the SO interaction is included (see Table II). This effect can be compared to that found for PbTe (Ref. 8) for the equivalent phonons, which lies around 5 cm⁻¹. Assuming that this effect is proportional to the sum of SO splittings of the valence electrons of cation and anion[8] (for values of atomic SO splittings, see Ref. 22) we predict, from the

TABLE II. Phonon frequencies at the zone center (in cm^{-1}) calculated for a **q** vector ∥ to trigonal axis.

	$E(TO)$	$A_1(LO)$
$p=0$ (no spin orbit)	73	153
$p=0$ (with spin orbit)	72	152
$p=2.1\times10^{21}$ holes/cm^3	73	115
Expt. (present work)	88	123
Expt.[a]	80	122

[a]Reference 21.

value of 5 cm^{-1} calculated for PbTe, 1.4 cm^{-1} for GeTe, compatible with the value of 1.3 cm^{-1} obtained in the calculations. The softenings induced by SO coupling for other phonons in the BZ are even smaller and thus will be henceforth neglected.

In Fig. 1 we can also appreciate the effect of hole doping on the dispersion relations. Without doping, the TO phonons are split by as much as 45 cm^{-1} on account of the electrostatic field induced by the large transverse ionic charges.[23] This effect is a nonanalytic function of wave vector $\boldsymbol{k}$: for $k\approx0$ the LO and TO frequencies depend on the direction of k. The corresponding discontinuities disappear in the doped material as the transverse charges are screened by the free holes: like in the cases of As, Sb, and Bi (Refs. 24 and 25) the optical phonons of the doped GeTe are split by the rhombohedral field into a singlet (LO) and a doublet (TO), the splitting amounting to 42 cm^{-1}, in agreement with measurements by Raman spectroscopy[21] and with our experimental results (see Table II and Sec. IV A). The individual calculated frequencies are, however, smaller than experimental results. The differences between the absolute values of calculated and measured frequencies is probably due to the employed local-density and pseudopotential approximations, or, to temperature effects resulting from anharmonic terms which we do not include in the present calculations. Similar behavior has been noticed for the lead chalcogenides where the calculated LO frequency of PbTe is 28 cm^{-1} lower than the measured one (see Fig. 3 of Ref. 8).

We should mention at this point that similar softenings of the phonons of semiconductors on heavy doping have been investigated earlier both experimentally and theoretically. Most recently the case of boron-doped diamond has been considered, in connection with the superconductivity observed in this material.[26,27] For a hole concentration similar to the one used here Boeri *et al.*[26] find for diamond a softening of the optical frequency at Γ of $\sim$20%. From Table II we estimate a doping induced softening of 15% for the LO phonon and 30% for the TO phonons at Γ. It has been pointed out that the strong phonon softening, in the case of diamond, is related to a strong hole-phonon interaction, probably also responsible for superconductivity.[28] Both ferroelectricity and superconductivity point to a strong carrier-phonon interaction in GeTe. Phonon softenings upon doping with boron have also been observed in Si.[29,30] *Ab initio* calculations of the effect of thermal electron-phonon excitations on the phonon spectrum of Si also indicate a strong carrie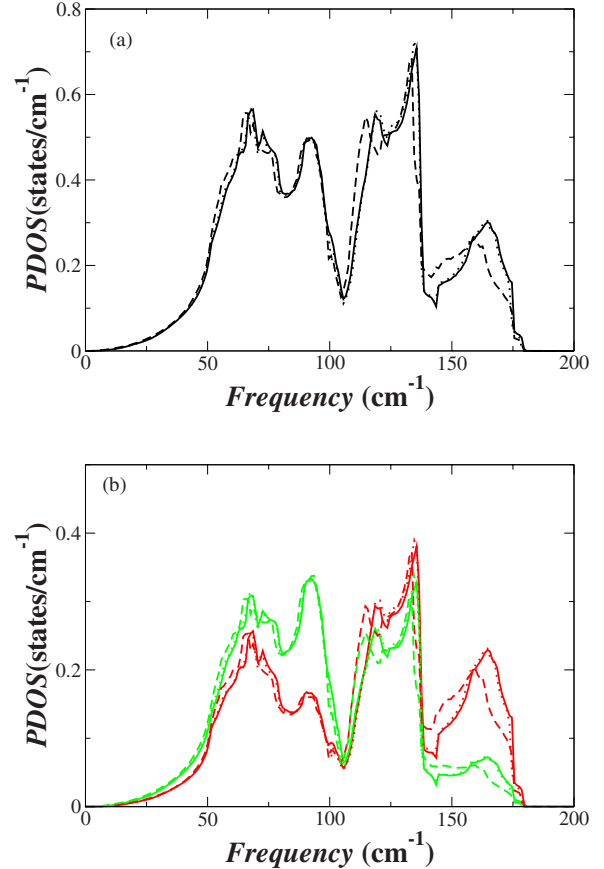r-induced softening of the transverse-acoustic phonons, especially at the edge of the Brillouin zone.[31] This softening is similar to that displayed in Figs. 1 and 2, although in this case only one type of carriers (holes) is involved.

We have calculated the phonon DOS and its projections on the Ge and Te atoms using the same procedure as in Refs. 7 and 8. The one-phonon DOS is shown in Fig. 2(a) for three different cases: undoped GeTe without SO interaction and with SO interaction included (note that the difference is hardly visible and, as already mentioned above, can be neglected) and GeTe with $p=2.1\times10^{21}$ holes/cm^3 (dashed line, no SO interaction). The presence of holes at the top of the valence band lowers all of the three bands in Fig. 2(a), corresponding to the softening of the dispersion relations in Fig. 1. Figure 2(b) displays the three DOSs of Fig. 2(a) projected on the two constituent atoms of α-GeTe. In Fig. 2 three bands are observed. They correspond to the acoustic phonons (from 0 to 110 cm^{-1}), the TO, and the LO phonons, respectively. Whereas in PbX (X=S,Se,Te) (Ref. 8) the TA band is almost exclusively Pb-like, Fig. 2(b) shows that for GeTe this band contains a strong mixture of Te and Ge vibrations ($\sim$60%−40%) whereby the heavier ion dominates, as expected for acoustic modes. The intermediate (TO) band contains a nearly equal mixture of vibrations of both atoms, with a slight predominance of the lighter one ($\sim$90%

FIG. 2. (Color online) (a) One-phonon DOS of α-GeTe calculated for an intrinsic sample (solid lines) without SO interaction, (dotted line) with SO interaction included, and (dashed line) for a sample with $p=2.1\times10^{21}$ holes/cm^3. (b) Projection of the DOS curves of (a) on Ge (red, black) and on Te (green, gray) atoms.

TABLE III. Values of the hole concentration of our samples in cm^{-3} as determined by various methods (see text). Also, values of the Sommerfeld coefficients γ in mJ/mol K^2 and $\beta = 2 \times 12/5 \pi^4 R / \theta_{Debye}^3$ in mJ/mol K^4 are given as well as the value of C_p/T^3 at the maximum in mJ/mol K^4. A blank signifies that a value is not available. The values from Ref. 4 are also cited for comparison.

Sample	p_H	γ	β	C_p/T^3_{max}	p_γ	γ_{op}
Bevolo	8×10^{19}	0.554(3)	0.307(1)	0.640(2)	8×10^{19}	
CG1	1.6×10^{21}	1.66(9)	0.380(9)	0.663(2)	1.2×10^{21}	
CG2		1.57(2)	0.368(3)	0.663(2)	1×10^{21}	1.5×10^{21}
CG3		1.19(2)	0.339(2)	0.658(2)	4×10^{20}	
Alfa		1.45(4)	0.358(3)	0.656(2)	8×10^{20}	

-10%). The LO band is clearly dominated by Ge vibrations ($\sim 30\% - 70\%$) as expected. All bands are lowered in the heavily p-doped material with respect to the undoped ones, as expected from the dispersion relations in Fig. 1. This lowering results in an increase in the maximum of $C_{v,p}$ vs T found at ~ 16 K, as will be discussed in Sec. IV.

IV. EXPERIMENTAL PROCEDURE AND RESULTS

A. Samples and sample characterization

Most of the measurements reported here were performed on wafers of a coarse polycrystalline ingot piece grown by the Bridgman technique in a quartz ampoule.[32] The ingot diameter was about 10 mm. We cut from it several wafers perpendicular to the growth axis, about 0.8 mm in thickness. The wafer measured by us will be labeled GeTe-CG. We also measured the heat capacity of commercial samples (99.999% purity, Alfa Aesar, Karlsruhe, Germany) consisting of small crystalline chips about 1 mm in size. Several chips weighing a total of ~ 23 mg were measured (they are labeled as Alfa-GeTe below). The results are compared to the data published by Bevolo *et al.*[4]

The wafers were characterized by Hall-effect measurements using the Van der Pauw technique.[33] No such measurements were possible for the granular Alfa Aesar sample. In this case, the hole concentration p was estimated from the linear-in-T term of the specific heat (Sommerfeld term, equal to γT) by comparing it to that reported in Ref. 4 for $p = 8 \times 10^{19}$ holes/cm^3. For this purpose we used the relation[34]

$$\gamma \propto m^* p^{1/3}, \tag{1}$$

where m^* is the effective band mass of the holes. We also estimated p in the CG2-GeTe sample from the plasma minimum in the ir reflection spectrum by comparing to similar data in Ref. 35. We found for this sample $p = 1.5 \times 10^{21}$ cm^{-3}. The values of p and γ for the samples under consideration and the estimated values of p are listed in Table III.

Table III displays the hole concentration of our two samples and that given by Bevolo *et al.*[4] as determined by Hall measurements (p_H) together with the concentration estimated from the ir reflectivity (γ_{op}) and those obtained from the measured values of γ. The latter were estimated by scaling the values of Bevolo *et al.*[4] using Eq. (1). In doing so, we have taken into account the fact that the effective mass m^*

increases with increasing p due to nonparabolicity of the bands. Since p_γ is proportional to $(m^*)^3$, its estimated value depends very critically on this nonparabolic increase, which is not accurately known at present. We have taken, for this increase, the values reported in Ref. 36: 24% for the Alfa Aesar sample and 32% for the CG sample with respect to the result of Bevolo *et al.*[4] In spite of some variations, the values of p listed in this table are adequate for the subsequent discussion of our heat-capacity measurements.

For the sake of completeness we also measured the Raman spectrum of the LO and TO phonons in our CG-GeTe sample. We found at 293 K $\omega_{LO} = 123$ cm^{-1} and $\omega_{TO} = 88$ cm^{-1}, in good agreement with the values reported in Ref. 37 for the same temperature.

B. Temperature dependence of the heat capacity

We display in Fig. 3 the heat capacity of GeTe measured below 5.5 K using the standard Sommerfeld plot (C_p/T versus T^2). The intercept of a linear fit with the ordinate yields the value of γ as listed in Table III.

Figure 4 shows the temperature dependence of C_p/T^3 measured for our two samples in the 2.5–30 K temperature range, together with the results of Bevolo *et al.*[4] The increase in C_p/T^3 seen below 5 K corresponds to the Sommerfeld term shown in Fig. 3. The most remarkable feature of Fig. 4 is the monotonic increase in C_p/T^3 observed with increasing p, which can be assigned to the frequency softening (cf. Fig. 1) and the corresponding downshift of the DOS [cf. Fig.
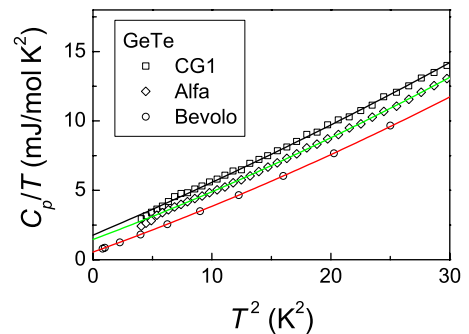

FIG. 3. (Color online) Sommerfeld plots of the heat capacities of our CG and Alfa samples of α-GeTe together with that for the sample of Bevolo *et al.* (Ref. 4). The γ values obtained from the intercept with the vertical axis are listed in Table III.
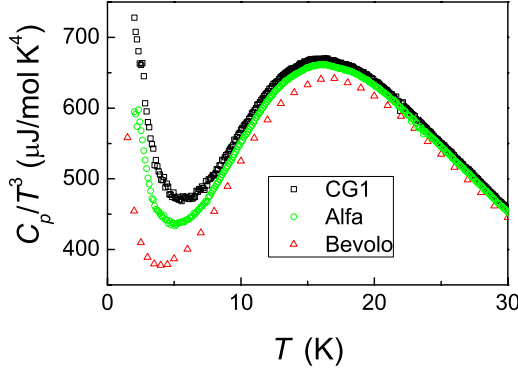
FIG. 4. (Color online) Measured temperature dependence of C_p/T^3 for the three samples of α-GeTe under consideration. Details for other samples are given in Table III. Note the increase of C_p/T^3 with increasing hole concentration (see Table III).

2(a)]. Notice also that our two samples exhibit this maximum at 15.8 K whereas Bevolo's maximum is found at 16.6 K. This shift can be assigned to the fact that the latter sample has a hole concentration over 1 order of magnitude lower than the former.

A simple relationship has been proposed earlier (Refs. 7 and 8) to relate the temperature of the maximum in C_p/T^3 to the phonon DOS. One first divides the temperature by 1.43 so as to convert T (in K) into cm^{-1}. Then one divides the obtained frequencies by 6.2. This procedure leads to the frequencies 68.5 cm^{-1} for our samples and 72 cm^{-1} for the sample of Bevolo *et al.*[4] The corresponding shift of 3.5 cm^{-1} agrees with that observed for the first TA peak in the DOS. The position of this peak, 70 cm^{-1}, also agrees with the average position estimated by the procedure followed above.

Figure 5 displays the temperature dependence of C_v/T^3 ($\sim C_p/T^3$) calculated for several different concentrations (p =0, 0.5×10^{21}, 1.0×10^{21}, and 2.1×10^{21} cm^{-3}). Notice that the effect of SO coupling, as implemented for the undoped sample, is small and we have not implemented it for doped GeTe. Hence, in the latter case we should compare it to the undoped calculation without SO interaction. We did not no-
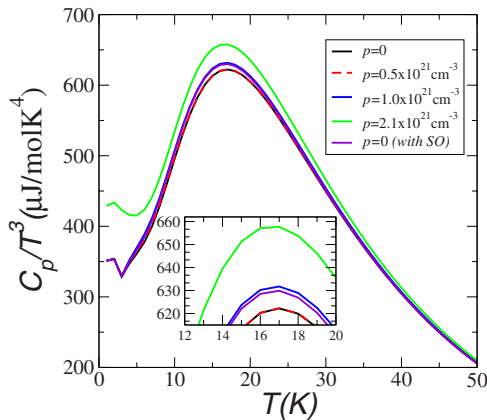

FIG. 5. (Color online) Calculated temperature dependence of C_v/T^3 for an undoped α-GeTe sample (with and without SO splitting) and for a sample with $p=0.5 \times 10^{21}$, 1.0×10^{21}, and 2.1×10^{21} cm^{-3} (without SO splitting).
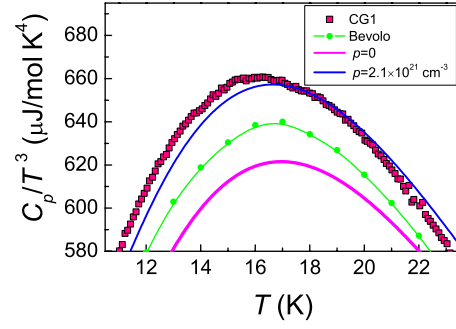

FIG. 6. (Color online) Heat capacity divided by T^3 measured for samples (Bevolo and our data CG1) compared to calculations with $p=0$ and $p=2.1 \times 10^{21}$ cm^{-3} without SO coupling.

tice much of a change for the light doping case ($p=0$, 0.5×10^{21} cm^{-3}). However, as expected, the increase in doping concentration leads to a monotonic increase in the maximum of C_v/T^3. As seen in Fig. 5, we found an increase in the maximum of 0.2% and 0.6% for $p=1.0 \times 10^{21}$ and 2.1×10^{21} holes/cm^3, respectively. The results agree rather well with the 0.5% measured for the CG sample, especially when one considers that this sample has a doping of about 1.5×10^{21} cm^{-3}. The shift in the calculated position of the maximum with doping is also close to the measured one.

It is of some interest to compare the small effect of the SO interaction shown in Fig. 5 to that calculated for PbTe. In Ref. 8 we proposed a perturbation expansion of the SO effect as a function of the strength of the SO splittings of the p valence electrons of Pb and Te. We use the same expression replacing the SO splitting of Pb (1.26 eV, cf. Ref. 22) by that of Ge (0.22 eV, cf. Ref. 22) and predict an effect of the SO coupling of 4% for the maximum of C_v/T^3 in α-GeTe (as opposed to 20% for PbTe). The effect observed in Fig. 5 is about 2%, somewhat smaller than the rough estimate carried over from the PbTe.

We conclude by displaying in Fig. 6 the temperature dependence of C_p as measured by us, Bevolo *et al.*,[4] and Zhdanov,[38] compared to our *ab initio* calculations of C_v up to 300 K. Our measurements up to 150 K, from which the Sommerfeld term has been subtracted, agree within error, with those of Zhdanov. Between 150 and 300 K, Zhdanov's data lie above the calculations. In order to ascertain whether this discrepancy is due to the difference between C_p and C_v we use the expression[39]

$$C_p(T) - C_v(T) = \alpha_v^2(T) B V_{\text{mol}} T, \qquad (2)$$

where $\alpha_v(T)$ is the temperature-dependent coefficient of the volume thermal expansion, B is the bulk modulus, and V_{mol} is the molar volume.

We have evaluated Eq. (2) at 300 K using $\alpha_v=5.60 \times 10^{-5}$ K^{-1} (Ref. 40), $B=49.9$ GPa (Refs. 20 and 23), and a molar volume of 32.3 cm^3. We find a thermal-expansion contribution to C_p-C_v of ~ 1.5 J/mol K at 300 K, which is by a factor of ~ 2.5 smaller than the value required to bring Zhdanov's data (C_p) to agree with the calculation (C_v). In order to clarify this matter, measurements should be repeated in the temperature range 150–300 K (Fig. 7).
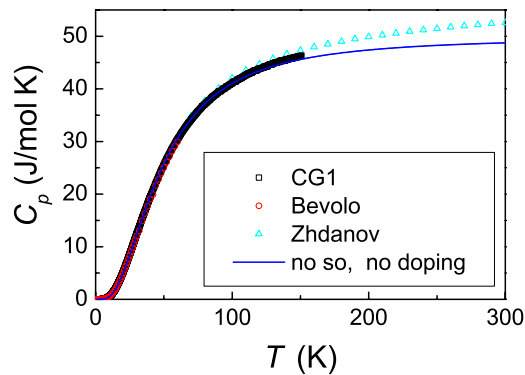
FIG. 7. (Color online) Measured heat capacity of several α-GeTe samples in the 3–300 K range. The black solid line represents our *ab initio* calculations. The linear dependence in Zhdanov's data for $T < 150$ K corresponds to the thermal-expansion effect.

V. CONCLUSIONS

We have presented a detailed experimental and theoretical investigation of lattice dynamics and heat capacity of α-GeTe. In contrast to previously reported results for other IV-VI materials,[8] we found that the inclusion of spin-orbit coupling has a small effect on the calculated phonon fre-

quencies and consequently on the heat capacity. On the other hand, we found that ignoring nonstoichiometry effects of GeTe leads to discrepancies between the calculated and the measured C_p/T^3. These can be resolved by taking into account the existence of free holes which lead to an increase of C_p/T^3. Such increase was found to be due to phonon frequency softening and the corresponding downshift of the density of phonon states.

*Corresponding author. r.kremer@fkf.mpg.de

[1] K. M. Rabe and J. D. Joannopoulos, Phys. Rev. Lett. **59**, 570 (1987).

[2] K. M. Rabe and J. D. Joannopoulos, Phys. Rev. B **36**, 6631 (1987).

[3] J. Goldak, C. S. Barret, D. Innes, and W. Youdelis, J. Chem. Phys. **44**, 3323 (1966).

[4] A. J. Bevolo, H. R. Shanks, and D. E. Eckels, Phys. Rev. B **13**, 3523 (1976).

[5] R. A. Hein, J. W. Gibson, R. Mazelsky, R. C. Miller, and J. K. Hulm, Phys. Rev. Lett. **12**, 320 (1964).

[6] L. Finegold, Phys. Rev. Lett. **13**, 233 (1964).

[7] M. Cardona, R. K. Kremer, R. Lauck, G. Siegle, J. Serrano, and A. H. Romero, Phys. Rev. B **76**, 075211 (2007).

[8] A. H. Romero, M. Cardona, R. K. Kremer, R. Lauck, G. Siegle, J. Serrano, and X. C. Gonze, Phys. Rev. B **78**, 224302 (2008).

[9] K. C. Mills, *Thermodynamic Data for Inorganic Sulphides, Selenides and Tellurides* (Butterworths, London, 1974).

[10] X. Gonze, J.-M. Beuken, R. Caracas, F. Detraux, M. Fuchs, G.-M. Rignanese, L. Sindic, M. Verstraete, G. Zerah, F. Jollet, M. Torrent, A. Roy, M. Mikami, Ph. Ghosez, J.-Y. Raty, and D. C. Allan, Comput. Mater. Sci. **25**, 478 (2002); The ABINIT code results from a common project of the Université Catholique de Louvain, Corning, Incorporated, and other collaborators. http://www.abinit.org

[11] X. Gonze, G.-M. Rignanese, M. Verstraete, J.-M. Beuken, Y. Pouillon, R. Caracas, F. Jollet, M. Torrent, G. Zerah, M. Mikami, P. Ghosez, M. Veithen, J. Y. Raty, V. Olevano, F. Bruneval, L. Reining, R. Godby, G. Onida, D. R. Hamann, and D. C. Allan, Z. Kristallogr. **220**, 558 (2005).

[12] For a review, see, S. Baroni, S. de Gironcoli, A. Dal Corso, and

P. Giannozzi, Rev. Mod. Phys. **73**, 515 (2001).

[13] X. Gonze, Phys. Rev. B **55**, 10337 (1997).

[14] X. Gonze and C. Lee, Phys. Rev. B **55**, 10355 (1997).

[15] C. Hartwigsen, S. Goedecker, and J. Hutter, Phys. Rev. B **58**, 3641 (1998).

[16] S. Goedecker, M. Teter, and J. Hutter, Phys. Rev. B **54**, 1703 (1996).

[17] H. J. Monkhorst and J. D. Pack, Phys. Rev. B **13**, 5188 (1976).

[18] M. Methfessel and A. T. Paxton, Phys. Rev. B **40**, 3616 (1989).

[19] A. Ciucivara, B. R. Sahu, and L. Kleinman, Phys. Rev. B **73**, 214105 (2006). This work was performed without spin-orbit interaction.

[20] A. Onodera, I. Sakamoto, Y. Fujii, N. Môri, and S. Sugai, Phys. Rev. B **56**, 7935 (1997).

[21] K. Andrikopoulos, S. Yannopoulos, G. Voyiatzis, A. Kolobov, M. Ribes, and J. Tominaga, J. Phys.: Condens. Matter **18**, 965 (2006).

[22] F. Herman and S. Skillman, *Atomic Structure Calculations* (Prentice Hall, Englewood Cliffs, NJ, 1963).

[23] R. Shaltaf, E. Durgun, J.-Y. Raty, Ph. Ghosez, and X. Gonze, Phys. Rev. B **78**, 205203 (2008).

[24] L. E. Diaz-Sanchez, A. H. Romero, M. Cardona, R. K. Kremer, and X. Gonze, Phys. Rev. Lett. **99**, 165504 (2007).

[25] J. Serrano, R. K. Kremer, M. Cardona, G. Siegle, L. E. Diaz-Sanchez, and A. H. Romero, Phys. Rev. B **77**, 054303 (2008).

[26] L. Boeri, J. Kortus, and O. K. Andersen, Sci. Technol. Adv. Mater. **7**, S54 (2006).

[27] M. Hoesch, T. Fukuda, J. Mizuki, T. Takenouchi, H. Kawarada, J. P. Sutter, S. Tsutsui, A. Q. R. Baron, M. Nagao, and Y. Takano, Phys. Rev. B **75**, 140508(R) (2007).

[28] M. Cardona, Sci. Technol. Adv. Mater. **7**, S60 (2006).

[29] L. Pintschovius, J. A. Vergés, and M. Cardona, Phys. Rev. B **26**, 5658 (1982).

[30] F. Cerdeira, T. Fjeldly, and M. Cardona, Phys. Rev. B **8**, 4734 (1973).

[31] V. Recoules, J. Clerouin, G. Zerah, P. M. Anglade, and S. Mazevet, Phys. Rev. Lett. **96**, 055503 (2006).

[32] E. Schönherr, in *Crystals—Growth, Properties, and Applications*, edited by H. C. Freyhardt (Springer, Berlin, 1980), Vol. 2, pp. 51–118.

[33] L. Van der Pauw, Philips Res. Rep. **13**, 1 (1958).

[34] N. W. Ashcroft and N. D. Mermin, *Solid State Physics* (Holt, Rinehart and Winston, New York, 1976).

[35] I. A. Drabkin, T. B. Zhukova, I. V. Nel'son, and L. M. Syoseva, Inorg. Mater. **15**, 936 (1979).

[36] J. E. Lewis, Phys. Status Solidi B **59**, 367 (1973).

[37] E. F. Steigmeier and G. Harbeke, Solid State Commun. **8**, 1275 (1970).

[38] V. M. Zhdanov, Russ. J. Phys. Chem. **45**, 1357 (1971).

[39] R. K. Kremer, M. Cardona, E. Schmitt, J. Blumm, S. K. Estreicher, M. Sanati, M. Bockowski, I. Grzegory, T. Suski, and A. Jezowski, Phys. Rev. B **72**, 075209 (2005).

[40] H. Wiedemeier and P. A. Siemers, Z. Anorg. Allg. Chem. **431**, 299 (1977).